

A simple approach for FEM simulation of Mode I cohesive crack growth in glued laminated timber under short-term loading

Stefania Fortino, Giuseppe Zagari, Antonio Lorenzo Mendicino and Gerhard Dill-Langer

Summary. This paper presents a simple computational approach for the analysis of Mode I short-term cohesive crack growth in glued laminated timber (glulam). The crack growth simulation is performed by using the cohesive elements of Abaqus finite element code in the fracture zone and a suitable exponential damage law. The optimal parameters for the damage law are determined by means of a parametric study involving a certain number of nonlinear analyses for monotonically proportional loads. The numerical method is described through the analysis of a wedge-splitting specimen under Mode I crack propagation taken from the literature. A key point of the paper is the simulation of short-term cohesive crack growth in modified double cantilever beam (DCB) glulam specimens prepared and tested within the present research. The influence of different adhesives in the fracture behaviour of wooden bond-lines is studied.

Key words: glulam, Mode I fracture, wedge-splitting specimen, modified DCB specimen, wooden bond-lines, crack growth, cohesive elements, FEM, Abaqus code

Introduction

The numerical analysis of crack propagation in glued laminated timber (glulam) structures is an important tool to assess the serviceability and the safety of these structures (Sjödén, 2008). Both the crack propagation system of wood and the used adhesives can affect the crack growth in glulam (Stanzl-Tschegg et al., 1995; de Moura et al., 2006; Dourado et al., 2008; Serrano, 2000; Simon & Valentin, 2003).

Glulam structural elements offer several advantages if compared to solid wood members and their manufacturing is significantly characterized by the adhesives production aimed to provide high-performance timber (George et al., 2003). The stress concentrations in glulam structures usually appear in the vicinity of glue-lines mainly due to the effect of lamination anisotropy and lay-up (Aicher & Dill-Langer, 2005), also under variable humidity conditions (Fortino et al., 2009; Zhou et al., 2010). On the other hand, relatively few scientific publications are available on both experimental and computational issues concerning fracture parameters of bond-lines in glued wooden products (see Simon & Valentin, 2000, 2003; Serrano & Gustafsson, 1999; Serrano, 2000, and related references). As discussed in (Serrano & Gustafsson, 1999), the strength of timber finger joints may be influenced by the brittleness of the bond-lines. This means that, in some cases, the optimal use of adhesives could help to prevent or, at least, to reduce the formation of cracks. In general, more research effort is needed to better understand the influence of different types of adhesives in the performance of glulam structures. In fact, the mechanical properties

of adhesives, as well as their performance on bonded wood joints are still a challenging research topic (see Konnerth et al., 2006; Clauß et al., 2011, and related references).

At the macroscopic level of structures wood is usually described as a continuum, homogeneous and orthotropic material. The material directions are identified by the growth mechanism in circular increments which produces the annual growth rings in the cross sectional plane and mainly longitudinally oriented cells called tracheids at the microscopic level (Hanhijärvi, 1995). The radial (R) axis is oriented in the direction of rays, the tangential (T) axis in the direction of the annual rings and the longitudinal (L) axis in the direction of the tracheids. The principal systems of crack growth are indicated as TL, RL, LR, TR, RT and LT where the first letter indicates the direction of the normal to the crack plane and second letter refers to the direction of crack growth (Silva et al., 2006).

Fracture processes in glulam are often caused by a combination of Mode I (opening mode) and Mode II (in-plane shear mode) loading (Sjödin, 2008). More research effort on both these fracture modes in glulam elements can help to better understand the cracking phenomena in timber structures as, for example, timber connections. In the present paper the attention is focused on the opening mode.

The short-term crack growth in different types of wood specimens under Mode I loading has been widely studied in the past literature for different crack propagation systems. In (Boström, 1994a,b) the effects of elasticity modulus, tensile strength, fracture energy and specimen size on the load-displacement curve were studied for a compact test (CT) specimen under opening mode. In Aicher (1994) a study on the Mode I critical strain energy release rate and the fracture energy in single edge notched beam (SENB) specimens in the RL crack configuration was carried out concluding that the fracture energy is quite independent of the initial crack length. In (Stanzl-Tschegg et al., 1995) the load-displacement curves of wedge-splitting specimens with RL and TL crack propagation systems of wood were studied experimentally as well as numerically.

The recent literature shows a growing use of Abaqus FEM code for the numerical analysis of various fracture mechanics problems in orthotropic solid wood for both Mode I and Mode II loading (see, among others, Dourado et al., 2008; de Moura et al., 2008; Silva et al., 2006; de Moura et al., 2006) also in the presence of different moisture levels (Vasic & Stanzl-Tschegg, 2007) and dynamics loads (Vasic et al., 2009). In particular, an advanced work on cohesive models for crack growth in wood under Mode I loading and on the evaluation of cohesive properties by an inverse method has been presented in (Dourado et al., 2008) for single edge notched beams (SENB) and in (de Moura et al., 2008) for double cantilever beam (DCB) specimens. In (Dourado et al., 2008) a method for evaluating the resistance-curves corresponding to the experimental load-displacement curves was also proposed by using the so-called equivalent LEFM approach (see also Morel et al., 2005). Furthermore, in (de Moura et al., 2008) a new data reduction scheme was presented in order to avoid the problems related to the crack monitoring during crack propagation. Finally, a recent numerical study by Schmidt & Kaliske (2009) for opening mode and shear mode in wood proposed an advanced interface element formulation including an anisotropic traction separation law and a coupling of failure modes suitable to be implemented into commercial FEM programs.

In the present work a simple computational approach for problems of Mode I short-term cohesive crack growth in glued laminated timber is presented which uses a specialized combination of tools of the Abaqus FEM code (Abaqus, 2008). Because of its simplicity, this method could be easily used as a further numerical tool within more general and

complex computational frameworks for wood modelling where also time-dependent and environmental effects are taken into account (Ormarsson, 1999; Fortino et al., 2009; Zhou et al., 2010). As pointed out in (Fragiacomo et al., 2011) a complete numerical model for calculation of moisture induced stresses perpendicular to grain in glulam under climate variations should also include the modelling of cracking in tension.

An other key point of this work is the application of the presented computational method to DCB glulam specially modified within this research to show cohesive crack propagation inside the bond-lines between wood adherents. The effect of different adhesives on the short-term fracture response of the specimens is investigated.

In Section 2 some generalities on the cohesive models for wood material are discussed. In the same section, to assess the performance of the proposed numerical approach, the wedge-splitting specimen in solid wood originally studied by Stanzl-Tschegg et al. (1995) is analyzed. Since for this test the direction of crack extension is known, the fracture process zone (FPZ) is described by using the cohesive elements available in Abaqus and a suitable exponential damage law defined on the basis of the load-displacement curve of the specimen. The parameters characterizing the damage curve are obtained by means of a parametric study performed by using several 3D nonlinear analyses solved by the Abaqus/Standard program and some Script tools (Abaqus, 2008). The wedge-splitting specimen is analyzed in the radial-longitudinal (RL) crack propagation system of wood. In Section 3 the proposed computational approach is used to analyze modified DCB glulam specimens under Mode I loading characterized by initial cracks forced to propagate inside the thicknesses of the bond-lines. The numerical results are in agreement with the experimental data. In Section 4 the conclusions on the obtained results are discussed and some suggestions for the future work are given.

A numerical approach for cohesive crack propagation in wood

Generalities on cohesive models for wood material

The crack growth in solid wood and glulam specimens subjected to short-term loading can be numerically simulated by using a nonlinear fracture mechanics (NLFM) approach and cohesive elements (Bazant & Planas, 1998; de Borst et al., 2004). The cohesive-zone (CZ) models were originally introduced by Barenblatt (1962) and Dugdale (1960) for elastic-plastic fracture in ductile metals, and for quasi-brittle materials by Hillerborg et al. (1976) in the so-called fictitious crack model.

The phenomenon of onset of Mode I crack growth and the consequent damaging in wood is described in detail in (Boström, 1994a). During the loading process, the load-displacement relationship remains linear elastic in the first part of the ascending branch of the curve. As the load approaches a critical value corresponding to the first damage phenomena into the wood (microcracks and bridging), some damage appears in the whole specimen. When the maximum load is reached, a localized fracture process zone (FPZ) starts to develop. Then, all additional displacements take place in the FPZ while the material outside this zone is unloaded elastically. In the cohesive zone models, the degrading mechanisms in the fracture process zone are assumed to hold into a discrete line or plane and are represented by a stress-displacement relationship which is a damage law and defines the softening behaviour of the material. For quasi-brittle materials as wood, the most used damage laws are linear, bi- or trilinear as well as exponential. As pointed out in (Boström, 1994a), the parameters characterizing the stress-displacement curve of a CZ model are the tensile strength and the work of separation or fracture energy, which is

defined as the work needed to generate a unit area of fully developed crack (see also Bazant & Planas, 1998). Then, the mechanical properties outside the fracture process zone can be defined by a usual stress-strain curve while inside the FPZ a stress-displacement curve has to be used.

In the case of crack path known *a-priori*, as for the problems analyzed in this paper, the cohesive behaviour in the fracture process zone can be defined in terms of a traction-separation law and the failure of the elements is characterized by a progressive degradation of the material stiffness which is driven by a damage process.

In this paper the cohesive elements available in Abaqus 6.8-2 (Abaqus, 2008) have been chosen to model the fracture process zone in both solid wood and glulam. To simulate the cohesive crack growth in wood, a damage initiation criterion of maximum stress, a displacement-based damage evolution criterion with exponential softening (Camanho & Davila, 2002) and a traction type mixed mode ratio have been used. By referring to the notation reported in (Abaqus, 2008), the following cohesive parameters characterizing the exponential law have been chosen: *a*) maximum nominal traction stress T_{\max} , after that the damage starts, *b*) maximum separation displacement δ_{\max} , after that the element does not contribute anymore to stiffness, and *c*) damage parameter α as exponent of the exponential law.

The cohesive parameters are selected through a procedure of parametric identification performed by using both the Riks analysis (Riks, 1979) of Abaqus/Standard and a suitable Abaqus Script. The Riks nonlinear static solver, also known as arc-length method, is chosen in order to avoid the typical stability problems of explicit solvers. Following (Abaqus, 2008), parametric studies permit to generate the results of several analyses that differ only in the values of some of the parameters. These studies can be performed by preparing a user-developed Script file containing Python instructions (Lutz, 1996). As shown in the next sections, a certain number of nonlinear analyses for the monotonically proportional loads acting on the analyzed wood specimen are automatically conducted by a suitable Script. In these analyses the loads are such as to reproduce the value of the cohesive fracture energy (Bazant & Planas, 1998). The parameter identification problem is solved on the basis of the curve which minimizes the difference between the calculated FEM curve and the experimental one. The minimization problem is based on the simple least square analysis. For general cases more complex statistical approaches can be used (Maier et al., 2006). For wood material, inverse methods which combine experimental data and a genetic algorithm were proposed in (Dourado et al., 2008; de Moura et al., 2008).

Case study: analysis of the Stanzl-Tschegg et al. wedge-splitting specimen

To describe the computational approach proposed in this research, the wedge-splitting specimen originally studied in (Stanzl-Tschegg et al., 1995) for Mode I loading has been analyzed (see Fig. 1). The specimens tested by Stanzl et al. were in spruce wood and their shapes were the same as in Tschegg's patents (see references in Stanzl-Tschegg et al., 1995). After drying to a moisture content of 12-13 %, the specimens were conditioned at a temperature $T = 20^{\circ}\text{C}$ and relative humidity $\text{RH} = 65\%$ to equilibrium moisture content. The crack growth in both the crack propagation systems TL and RL was studied. The results of fracture tests were registered as load-displacement curves. The computational FEM simulation of crack growth was performed in 2D on the basis of bi-linear damage laws. Stanzl-Tschegg et al. studied the influence of ligament length and of specimen

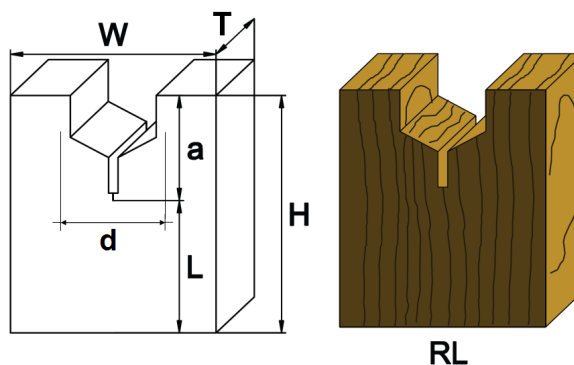


Figure 1. The Stanzl-Tschegg et al. wedge splitting specimen. Left: geometry. Right: RL crack propagation system. T = specimen thickness (variable), W = specimen width = 100 mm, L = ligament length (variable), a = 46 mm, d = opening displacement.

Table 1. Material properties used for the analysis of the Stanzl-Tschegg et al. specimen.

E_R	E_T	E_L	G_{RT}	G_{RL}	G_{TL}	ν_{RT}	ν_{RL}	ν_{TL}
[MPa]	[MPa]	[MPa]	[MPa]	[MPa]	[MPa]	[-]	[-]	[-]
900	500	12000	40	700	700	0.558	0.038	0.015

thickness on the specific fracture energy concluding that there is no size effect for ligament lengths more than 70 mm and specimen thicknesses above 30 mm. For example, the fracture energy remains essentially constant and equal to 240 [J/m²] for the RL crack propagation system. In the present work the RL specimen is studied and the chosen specimen thickness is $T=40$ mm.

The 3D Abaqus model of the Stanzl-Tschegg et al. specimen in RL crack propagation system with cohesive elements is shown in Fig. 2. The specimen is loaded in opening mode as done in (Stanzl-Tschegg et al., 1995). A quarter of the structure is analyzed. Material orientations are given to the wood sections in order to describe the crack propagation system. The position of the L axis (longitudinal direction) gives the position of the pith, that is the center of the annual rings, while the directions of R and T (radial and tangential directions) refer to the material orientation in the cross-sectional plane. In the Abaqus model, rectangular coordinate systems RTL are used since the pith is assumed to be located quite far from the structure. In cases with pith located inside or very close to the lamella, a more accurate approach needs the definition of a cylindrical material coordinate system as done in (Fortino et al., 2009; André, 2007). The influence of cylindrical coordinate systems on the stress calculation has been discussed in detail in (Aicher & Dill-Langer, 2005). The wood material parameters used for the analysis are listed in Table 1.

The COH3D8 8-node three-dimensional cohesive elements are chosen. Hexahedral quadratic brick elements C3D20 are used for meshing the wood parts adjacent to the cohesive elements. In the Abaqus models analyzed in this work, the cohesive element zones are attached to the rest of the structure by means of the constraint option "TIE" of Abaqus/CAE. This approach yields certain benefits not reachable by the use of shared nodes for more general analysis cases: b) an identical cohesive zone can be used for differ-

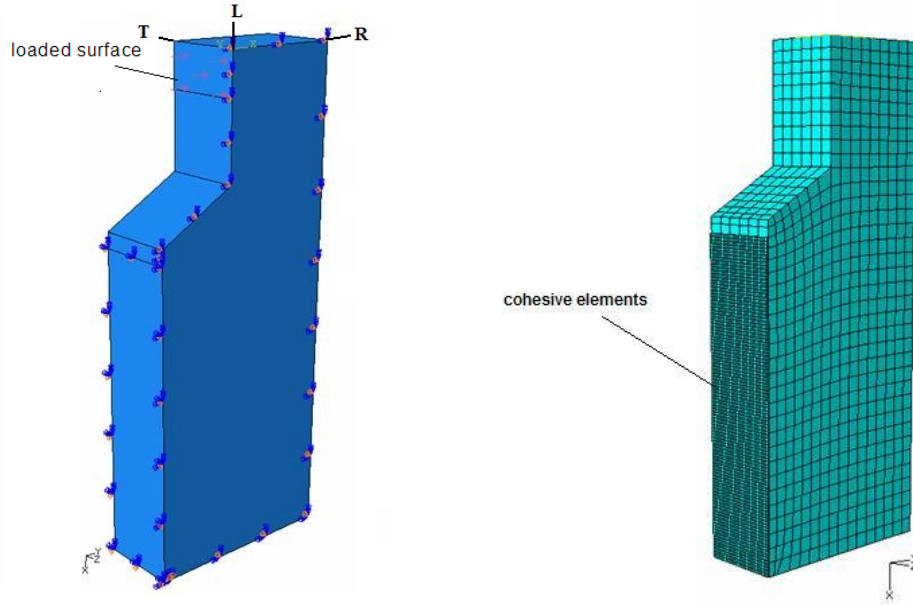


Figure 2. Wedge splitting specimen loaded in opening mode. Abaqus model (RL crack propagation system). Left: Geometry, load and boundary conditions. RTL = material coordinates. XYZ = global coordinates. Symmetry on planes XY and XZ. Right: Abaqus mesh and cohesive elements.

Table 2. Optimal cohesive parameters for the wedge splitting specimen and the value of the experimental fracture energy G_f for the RL crack propagation system.

	T_{\max} [MPa]	δ_{\max} [mm]	α [-]	G_f [J/m ²]
RL	2.660	0.495	0.490	240

ent parts and specimens containing cracks and this is beneficial in terms of comparability of results as well as modelling efficiency, b) in the case of glued specimens, more complex cohesive zone responses due for example to environmental effects can be assessed more easily when the cohesive zone region is separated from the parent region.

Several nonlinear analyses are conducted by using the Riks method of Abaqus/Standard for different combinations of cohesive parameters in order to choose the values to be used for the optimal interpolation of the experimental curves. During the nonlinear analysis for short-term test, the eventual viscoelastic effects related to the intrinsic nature of wood material (Hanhijärvi & Mackenzie-Helnwein, 2003) are assumed to be negligible.

In Table 2 the optimal parameters for the damage law obtained by the parametric analysis are listed. The numerical load-displacement curves are drawn in Fig. 3 and refer to the opening displacement of Fig. 1. These curves interpolate the experimental data described in (Stanzl-Tschegg et al., 1995). Fig. 4 shows the optimal exponential softening law used for the studied crack propagation system on the basis of the parametric analysis results. This softening law appears very suitable for nonlinear fracture mechanics (NLFM) analysis of wooden wedge-splitting specimens. The activation of the softening and the

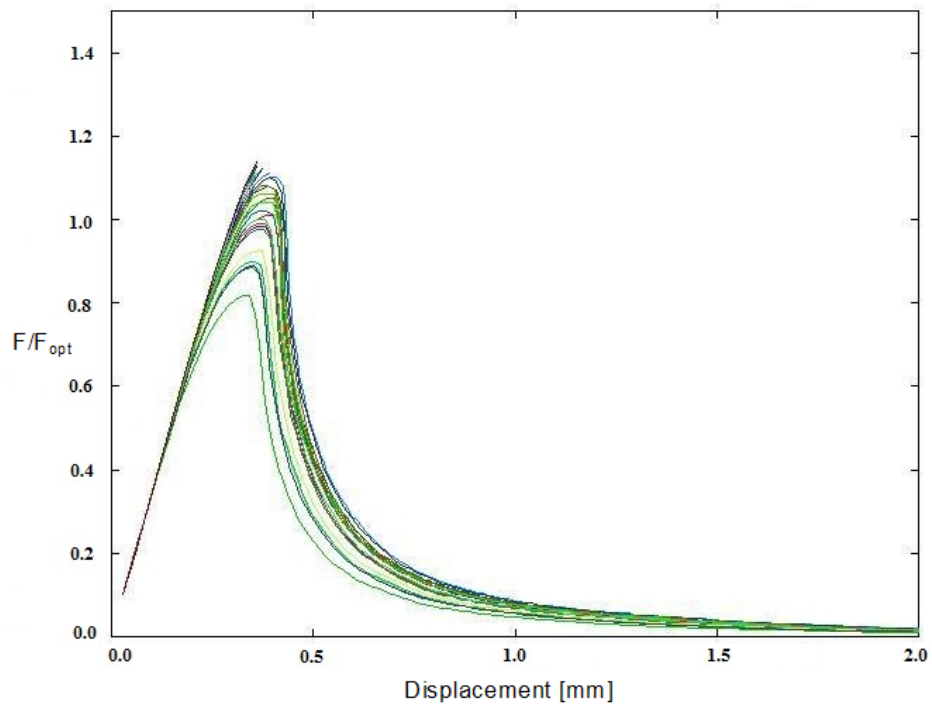


Figure 3. Wedge splitting specimen: Load-opening displacement curves from the parametric analysis. F_{opt} = peak load of the optimal load-displacement curve.

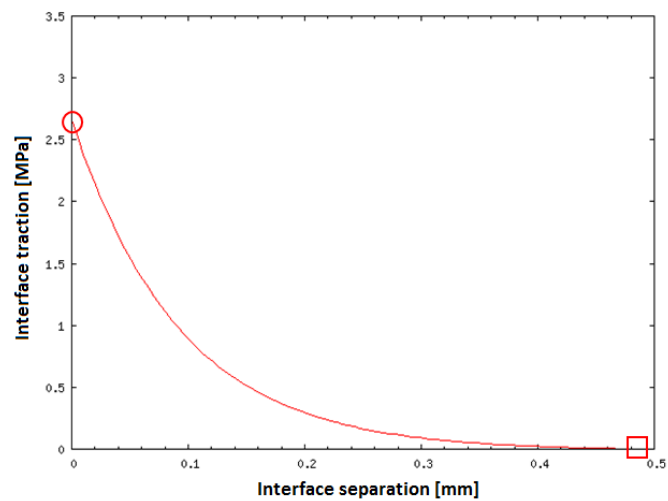


Figure 4. Optimal exponential law for the wedge splitting specimen. Circle point: damage initiation. Square point: starting of the separation.

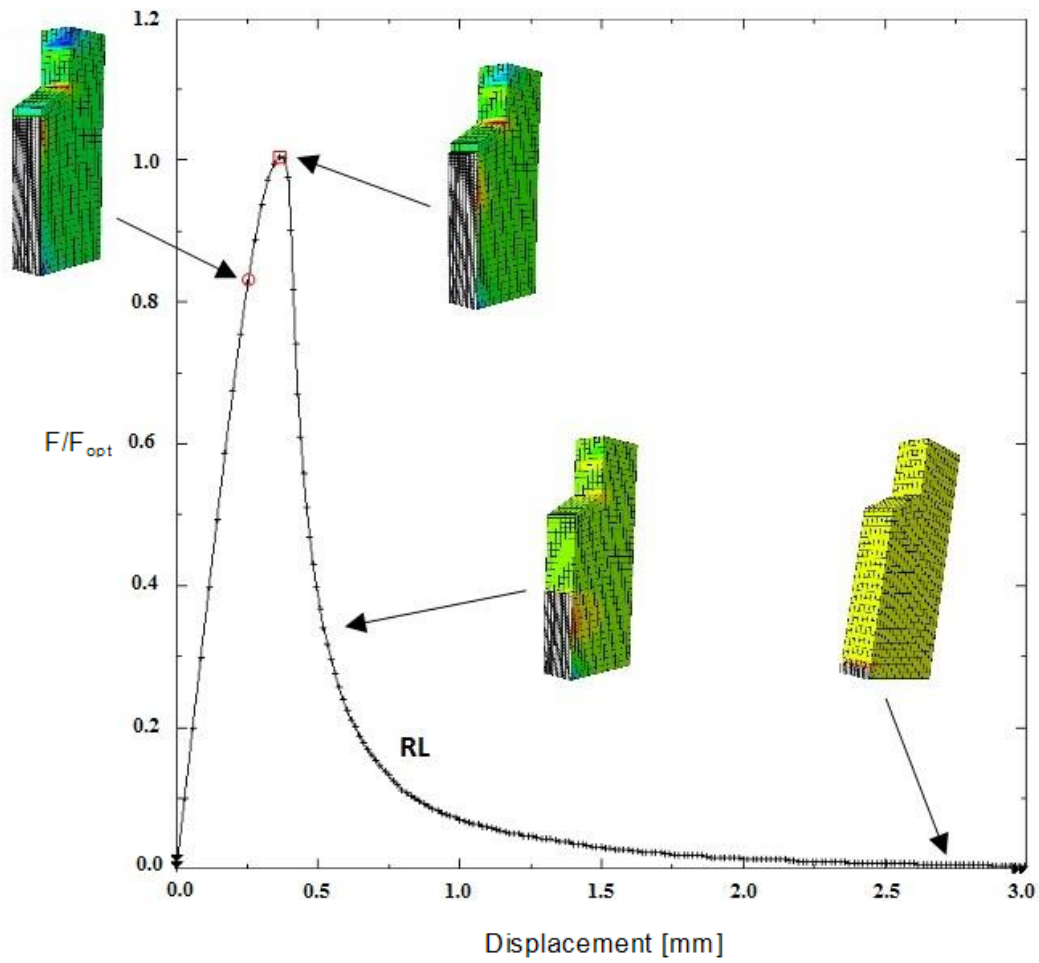


Figure 5. Optimal load-opening displacement curve for the wedge splitting specimen. Activation of crack growth and progress of the FPZ. F_{opt} = peak load of the optimal load-displacement curve. Circle point: damage initiation. Square point: starting of the separation.



Figure 6. Modified DCB specimen: view of the RL crack propagation system.

starting of opening, corresponding to the separation of cohesive elements from the rest of the meshed body, are shown in Fig. 5.

The presented computational approach can also be developed for the analysis of both solid wood and glulam cracked specimens under Mode II loading with known direction of crack growth by referring to the fracture energy values obtained from experimental tests. Different crack propagation systems can also be analyzed.

Analysis of modified DCB glulam specimens

The literature shows a lack of specimens suitable to study crack growth in glued laminated timber (Simon & Valentin, 2000, 2003). In general, the specimen geometries need to be modified for the inspection of fracture parameters at the interface between wood lamellas.

In the context of the present research, some modified double cantilever beam (DCB) glulam specimens in spruce wood have been realized by using different kind of adhesives between lamellas (see Figs 6 and 7). The wood substrates do not show defects. Each specimen is characterized by a chevron notch and an additional trapezoidal shaped groove aimed to force the crack growth inside the glue-line zone (see Fig. 8). The processes of drying and conditioning are the same as the ones described for the Stanzl et al. wedge-splitting specimen.

The modified DCB specimen is found to be suitable for *a*) solid wood and bond-lines and *b*) short-term tests aimed to evaluate the cohesive fracture energy. The measurement of crack propagation has been done by stepwise cut of strips of conducting paint. This kind of specimen can also be used for long-term tests under sustained loads.

Two types of modified DCB specimens with the same crack propagation system (RL) prepared with two different adhesives (named HBPU and MUF) have been tested and their load-displacement curves have been calculated both experimentally and numerically. HBPU is a hyperbranched polyurethane adhesive while MUF is a melamine-urea-formaldehyde adhesive. Usually MUF adhesives show higher stiffnesses if compared to polyurethane-based (PUR) adhesives (Konnerth et al., 2006; Clauß et al., 2011) but HBPU glues can be much stiffer than PUR glues (see Deka & Karak, 2009, and related

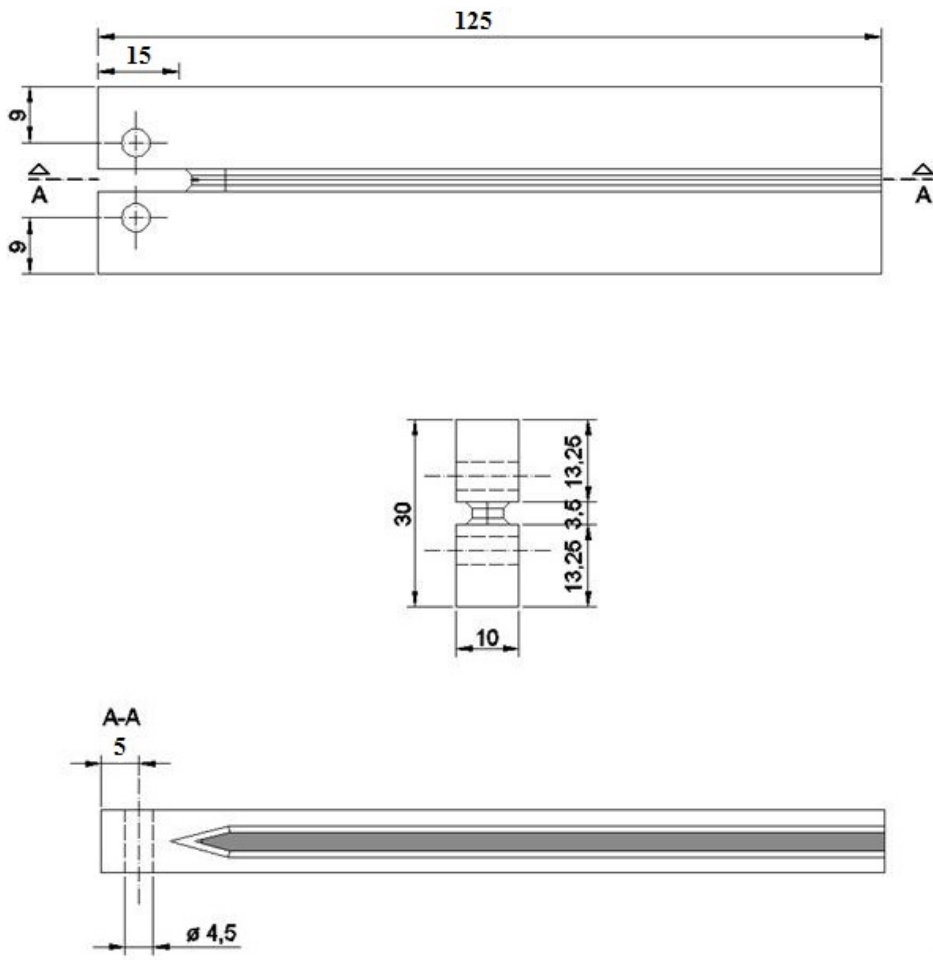


Figure 7. Modified DCB specimen: geometry (dimensions in mm).

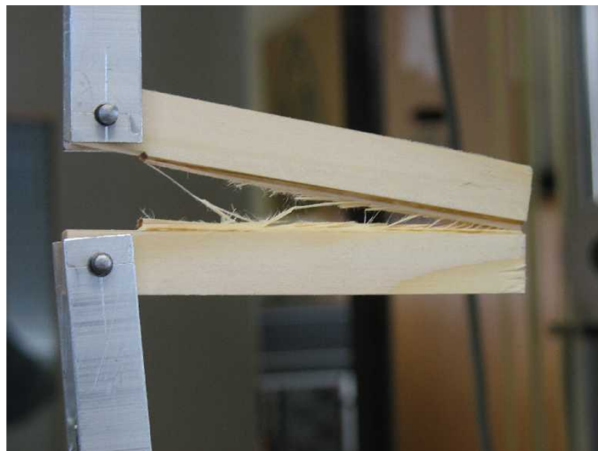


Figure 8. Modified DCB specimen. Fracture opening test.

Table 3. Modified DCB specimen: dimensions, loads and experimental values of the fracture energy. L_c =specimen length from the middle of the hole. a_c = notch length from the middle of the hole.

Specimen	HBPU	MUF
Specimen width B [mm]	4.73	4.53
Reduced specimen length L_c [mm]	120	120
Notch length a_c [mm]	10	10
Peak load F [N]	145.81	126.88
Fracture energy G_f [J/m ²]	164.74	141.37

Table 4. Mechanical properties used for the analysis of the modified DCB specimens.

E_R [MPa]	E_T [MPa]	E_L [MPa]	G_{RT} [MPa]	G_{RL} [MPa]	G_{TL} [MPa]	ν_{RT} [-]	ν_{RL} [-]	ν_{TL} [-]
900	600	13500	40	700	700	0.558	0.038	0.015

references).

The bond-lines between the wood adherent parts are characterized by material properties which depend not only on the bulk adhesive, but also on the wood part impregnated with the glue (interphase zone) and on possible mechanically weak boundary layers between the adhesive and the wood (Serrano, 2000). To accurately evaluate the material properties of the bond-lines, small scale tests should be performed as done, for example, in (Serrano & Gustafsson, 1999). In (Simon & Valentin, 2003) three possible debonding modes in the failure of the bond-line are assumed to hold: 1) the "adhesive" crack propagation holds along one of the two adhesive-substrate interfaces, 2) the "cohesive" growth develops inside the thickness of the adhesive layer and 3) the "interphase" extension involves a poor cohesion area very close to one of the two adhesive-substrate interfaces.

In the present paper the bond-line material is assumed to be isotropic and a general concept of crack growth across the bond-line is considered.

Within the present research, 4 specimens with HBPU adhesive and 5 specimens with MUF adhesive have been experimentally tested. The dimensions of the specimens and the values of loads, as well as the fracture energies computed during the experiments are reported in Table 3.

The fracture energy of the single specimen has been calculated from the related experimental curve (see Fig.10) by using the expression $G_f = I/[B(L_c - a_c)]$ where the integral I is calculated as: $I = \sum_{i=2..n} [(F_i + F_{i-1})/2](u_i - u_{i-1})$ being $(F_i, u_i), i = 1..n$ the experimental points of the nonlinear part of the load-displacement curve. This classical approach requires the monitoring of the crack length during propagation (Bazant & Planas, 1998). To avoid these difficult measurements, the approaches based on the beam theory are useful (Yoshihara, 2007). New methods based on both the beam theory and the concept of crack equivalent have been proposed in (Dourado et al., 2008) and (de Moura et al., 2008). These methods require the calculation of the specimen compliance and permit to obtain the critical energy release rate only as a function of the load-displacement data. However, further study is needed to evaluate the performance of this approach in

Table 5. Sets of parameters used for the parametric analysis of the specimens with HBPU and MUF adhesives.

HBPU	T_{\max} [MPa]	2.15	2.20	2.25
	δ_{\max} [mm]	0.08	0.12	0.16
	α [-]	0.6	1.0	1.4
MUF	T_{\max} [MPa]	1.75	1.787	1.825
	δ_{\max} [mm]	0.008	0.044	0.08
	α [-]	0.8	1.6	2.4

Table 6. Optimal damage parameters for the two modified DCB specimens.

	T_{\max} [MPa]	δ_{\max} [mm]	α [-]
HBPU	2.15	0.12	1.0
MUF	1.75	0.08	1.6

the presence of wooden bond-lines.

Simulation results: influence of the adhesives

The computational approach for short-term tests described in Section 2 has been used for analyzing the modified DCB specimen. Also for this example one quarter of the structure has been analyzed and the same options for the cohesive modelling used for the wedge-splitting example are chosen. The COH3D8 8-node three-dimensional cohesive elements for the interfaces and the hexahedral quadratic brick elements C3D20 for the wood parts are used. The material coordinates used in the Abaqus models refer to the RL crack propagation system (see Fig. 9). The material properties for wood used in the analysis are listed in Table 4. The Young modulus is the same for both HBPU and MUF adhesives ($E = 3000$ MPa). The values of the Young modules for the bond-lines are numerically obtained within the optimization problem and used to define the elastic properties of the cohesive elements. $E = 2650$ MPa for the specimen with HBPU glue and $E = 1650$ MPa for the one with MUF glue where found to be the optimal numerical values. The Poisson ratios are assumed to be $\nu = 0.3$ for both the adhesives. The smaller value obtained of E for the bond-line with MUF can be justified by the possible presence of weak interphase zones and weaker boundary layers. On the other hands, as hypothesized in (Clauß et al., 2011) the intracellular penetration of MUF adhesive in the interphase region could cause wood failure by making brittle the cell walls.

The two load-displacement experimental curves reported in the following are selected as representative curves in the range of the experimental results. After reaching the critical loads, the experimental load-displacement curves exhibit a quite unstable behaviour particularly evident in the MUF specimen (see experimental curves in Fig. 10). In addition, the short initial crack length used in the analysis can influence the sudden drop in the load-displacement curve of the MUF specimen. The experimental results points out some influence of the different adhesives in specimens having the same crack propagation system of wood (RL). In particular, the behaviour of the MUF curve seems to follows

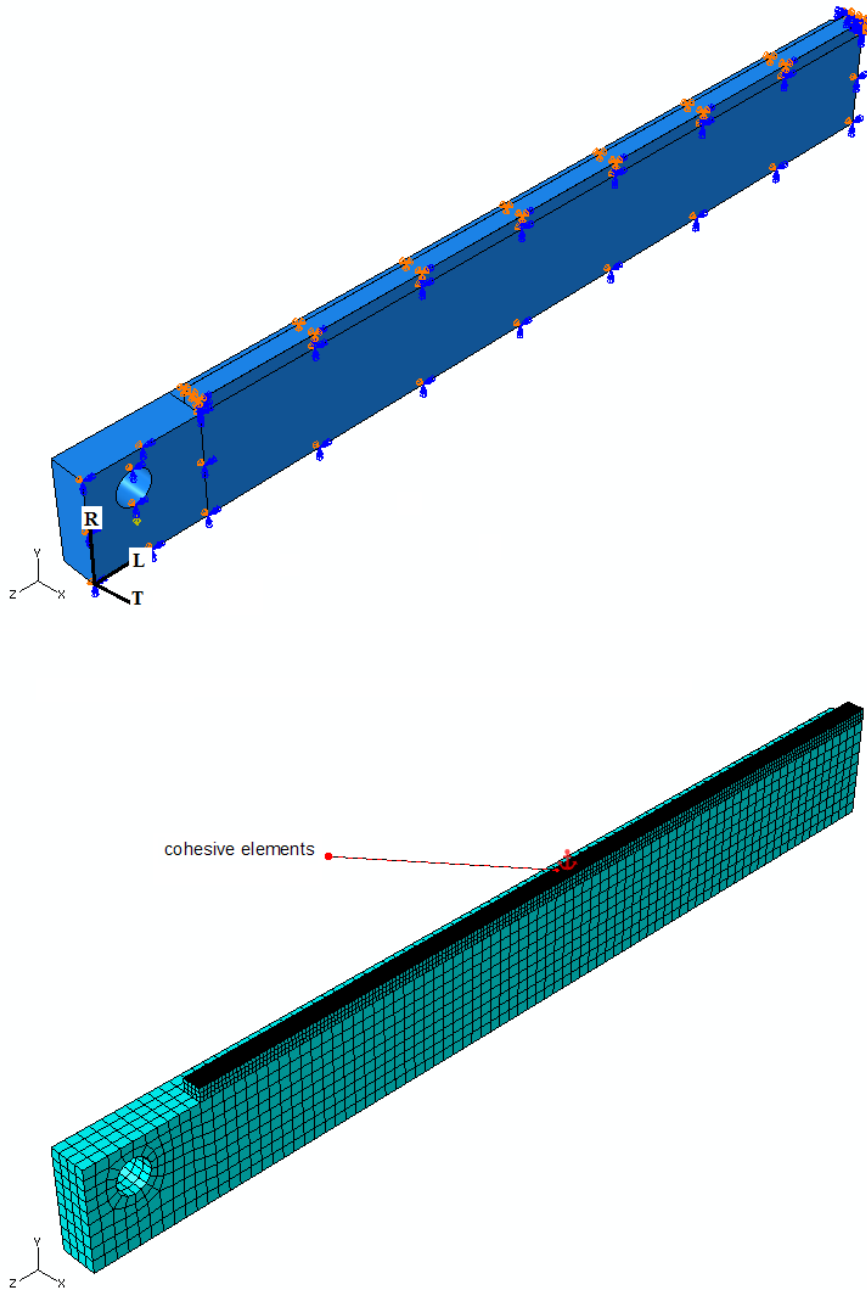


Figure 9. Modified DCB specimen. Top: Abaqus model. Bottom: mesh and cohesive elements by Abaqus. RL crack propagation system. RTL= material coordinates. XYZ= global coordinates. Symmetry on planes ZX and ZY.

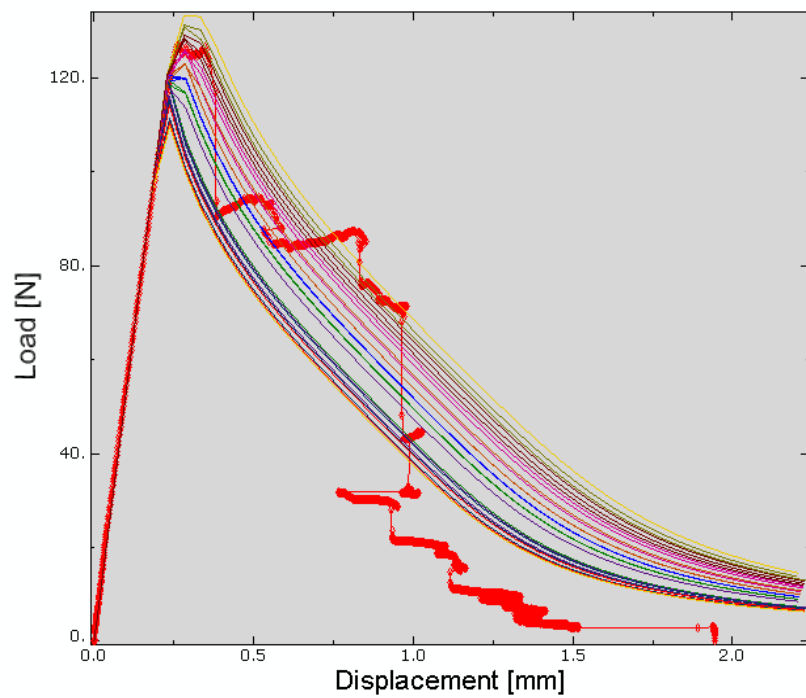
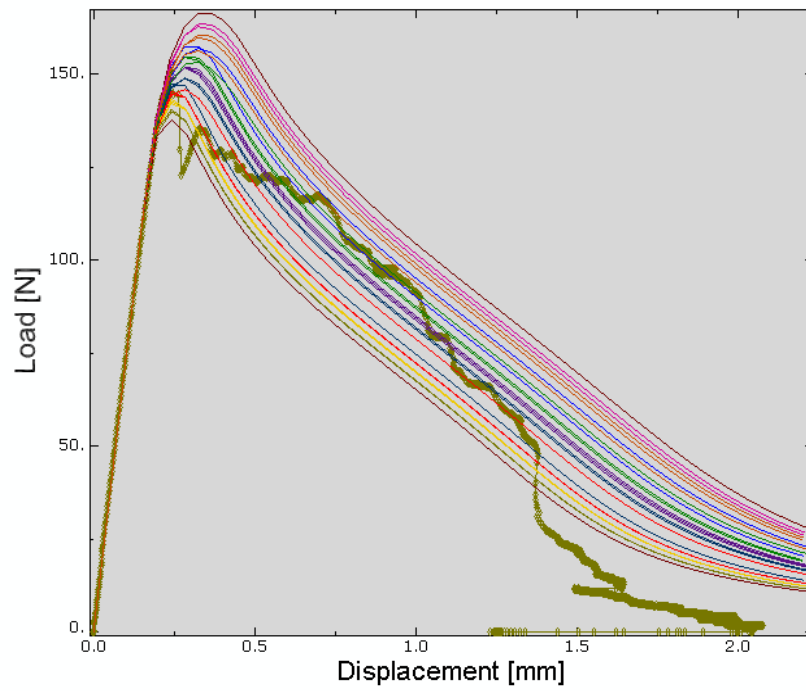


Figure 10. Numerical interpolation of experimental load-displacement curves of DCB specimen: results of the parametric analyses for HBPU specimen (top) and MUF specimen (bottom). Curves with symbols: experimental data.

a different damage law after a first descending branch. The HBPU load-displacement curve exhibits a more pronounced softening with respect to the other showing that more energy is needed for crack growth and, consequently, a higher fracture energy is required. This is probably due to the fact that usually the polyurethane-based adhesives show a more ductile behaviour compared to the MUF adhesives. As for the wedge-splitting specimen, a damage initiation criterion of maximum stress and a displacement-based damage evolution criterion with exponential softening have been used in the FEM modelling

Among the curves calculated by the parametric analysis, a best one has been chosen on the basis of a least squares measure. The parameters used for the analyses are listed in Table 5 and the optimal damage parameters in Table 6.

The obtained numerical curves for HBPU are in good agreement with the experimental ones (see Fig. 10). Although the MUF experimental curve is more unstable, the range of curves obtained by the parametric analysis appears suitable to interpolate it.

Conclusions and future work

In this paper a simple numerical approach for simulating the cohesive short-term crack propagation in timber structures has been presented.

The phenomenon of Mode I crack growth during short-term fracture tests in solid wood and across the bond-lines between lamellas in glulam is modelled by using the cohesive elements of Abaqus and suitable exponential damage laws obtained through parametric analyses driven by Abaqus Scripting studies. The used computational tools have been first described by analyzing the well-known Stanzl-Tschegg et al. wedge-splitting specimen.

The computational work has been supported by some experimental work conducted within the present research. In particular, modified double cantilever beam (DCB) specimens in glulam have been prepared, tested under Mode I loading and then computationally analyzed. Although the experimental load-displacement curves of these specimens show a quite unstable behaviour, the numerical results are in agreement with the experimental ones and some influence of different adhesives on fracture response of the tested specimens can be observed.

The numerical analysis is found to be suitable for both solid wood and glulam cracked specimens under short-term fracture tests in opening mode where the crack propagates in a known direction. This approach can be considered a useful numerical tool for the preparation of these kind of fracture tests.

To avoid the measurements of the crack length during crack growth for the calculation of the critical energy release rate, one of the equivalent crack methods proposed in the recent literature should be used to improve the performance of the presented approach.

The same computational tools can be used for analyzing cracked glulam specimens under shear loading. Also in this case the traditional specimens could be modified in order to show crack propagation across the bond-lines.

The presented computational approach, as well as the experimental work carried out in this research, can contribute to a better understanding of the crack growth phenomena in glued laminated timber.

Finally this approach appears easy to be used as a basic tool within more complex computational frameworks for the fracture analysis of glulam structures under variable environmental conditions.

Acknowledgement

The research work presented in this paper was funded by the European WoodWisdom-Net project Improved Moisture which is gratefully acknowledged. The authors would like to thank Mr. Maximilian Henning for his precious help in carrying out the experiments.

References

- Abaqus, a. (2008). *Abaqus/Standard, Theory Manual. Version 6.8*. Dassault Systèmes Simulia Corp. Providence, Rhode Island, U.S.A.
- Aicher, S. (1994). Bruchenergien, kritische energiefreisetzungsraten und bruchzähigkeiten von fichte bei zugbeanspruchung senkrecht zur faserrichtung. *Holz als Roh- und Werkstoff*, **52**, 361–370.
- Aicher, S., & Dill-Langer, G. (2005). Effect of lamination anisotropy and lay-up in glued-laminated timbers. *J. Struct. Eng.*, **131**(7), 1095–1103.
- André, J. (2007). Strengthening of timber structures with flax fibres. Tech. Rep. 61, Licentiate Thesis, Department of Civil, Mining and Environmental Engineering, Luleå University of Technology.
- Barenblatt, G. (1962). The mathematical theory of equilibrium cracks in brittle fracture. *Adv. Appl. Mech.*, **7**, 55–129.
- Bazant, Z., & Planas, J. (1998). *Fracture and size effect in Concrete and Other Quasibrittle Materials*. CRC Press.
- Boström, L. (1994a). The stress–displacement relation of wood perpendicular to the grain. part 1. experimental determination of the stress–strain relation. *Wood Science and Technology*, **28**, 309–317.
- Boström, L. (1994b). The stress–displacement relation of wood perpendicular to the grain. part 2. application of the fictitious crack model to the compact tension specimen. *Wood Science and Technology*, **28**, 319–327.
- Camanho, P., & Davila, C. (2002). Mixed-mode decohesion finite elements for the simulation of delamination in composite materials. Tech. Rep. NASA-TM-2002-211737, pp. 1-37.
- Clauß, S., Gabriel, J., Karbach, A., Matner, M., & Niemz, P. (2011). Influence of the adhesive formulation on the mechanical properties and bonding performance of polyurethane prepolymers. *Holzforschung*, doi-link: 10.1515.2011.095.
- de Borst, R., Gutierrez, M., Wells, G., Remmers, J., & Askes, H. (2004). Cohesive-zone models, higher-order continuum theories and reliability methods for computational failure analysis. *Int. J. Numer. Meth. Engng*, **60** (1), 289–315.
- de Moura, M., Morais, J., & Dourado, N. (2008). A new data reduction scheme for mode I wood fracture characterization using the double cantilever beam test. *Eng. Fracture Mech.*, **75**, 3852–3865.
- de Moura, M., Silva, M., de Morais, A., & Morais, J. (2006). Equivalent crack based mode II fracture characterization of wood. *Eng. Fracture Mech.*, **73**, 978–993.
- Deka, H., & Karak, N. (2009). Vegetable oil-based hyperbranched thermosetting polyurethane/clay nanocomposites. *Nanoscale Res Lett*, **4**, 758–765.

- Dourado, N., Morel, S., de Moura, M., Valentin, G., & Morais, J. (2008). Comparison of fracture properties of two wood species through cohesive crack simulations. *Composites Part A*, **39**, 415–427.
- Dugdale, D. (1960). Yielding of steel sheets containing slits. *J. Mech. Phys. Solids*, **8**, 100–108.
- Fortino, S., Mirianon, F., & Toratti, T. (2009). A 3d moisture-stress fem analysis for time dependent problems in timber structures. *Mech. Time-Depend. Mater.*, **13**(4), 333–356.
- Fragiacomo, M., Fortino, S., Tononi, D., Usardi, I., & Toratti, T. (2011). Moisture-induced stresses perpendicular to grain in cross-sections of timber members exposed to different climates. *Eng. Struct.*, **33**, 3071–3078.
- George, B., Simon, C., Properzi, M., Pizzi, A., & Elbez, G. (2003). Comparative creep characteristics of structural glulam wood adhesives. *Holz als Roh- und Werkstoff*, **61**, 79–80.
- Hanhijärvi, A. (1995). Modelling of creep deformation mechanisms in wood. Tech. Rep. Technical Report no 231, Dissertation, VTT Technical Research Centre of Finland.
- Hanhijärvi, A., & Mackenzie-Helnwein, P. (2003). Computational analysis of quality reduction during drying of lumber due to irrecoverable deformation. i: Orthotropic viscoelastic-mechanosorptive-plastic material model for the tranverse plane of wood. *J. Eng. Mech.*, **129**(9), 996–1005.
- Hillerborg, A., Modeer, M., & Petersson, P. (1976). Analysis of crack formation and crack growth in concrete by means of fracture mechanics and finite elements. *Cement Concrete Res*, **6**, 773–782.
- Konnerth, J., Jäger, A., Eberhardsteiner, J., Müller, U., & Gindl, W. (2006). Elastic properties and adhesive polymers. ii. polymer films and bond lines by means of nanoindentation. *J. Appl. Polymer Sci.*, **102**, 1234–1239.
- Lutz, M. (1996). *Programming Python*. O’Reilly and Associates, Inc.
- Maier, G., Bocciarelli, M., Bolzon, G., & Fedele, R. (2006). Inverse analyses in fracture mechanics. *Int. J. Fracture*, **138**, 47–73.
- Morel, S., Dourado, N., Valentin, G., & Morais, J. (2005). Wood: a quasibrittle material. r-curve behavior and peak load evaluation. *Int. J. Fracture*, **131**, 385–400.
- Ormarsson, S. (1999). Numerical analysis of moisture-related distortions in sawn timber. Tech. Rep. Technical Report Ny serie no 1531, Dissertation, Chalmers University of Technology.
- Riks, E. (1979). An incremental approach to the solution of snapping and buckling problems. *Int. J. Solids Structures*, **15**, 529–551.
- Schmidt, J., & Kaliske, M. (2009). Models for numerical failure analysis of wooden structures. *Eng. Struct.*, **31**, 571–579.
- Serrano, E. (2000). Adhesive joints in timber engineering - modelling and testing of fracture properties. Tech. Rep. Report TVSM-1012, Dissertation, Lund University, Division of Structural Mechanics.
- Serrano, E., & Gustafsson, J. (1999). Influence of bondline brittleness and defects on the strength of timber finger-joints. *Int. J. of Adhesion and Adhesives*, **19**(1), 9–17.

- Silva, M., de Moura, M., & Morais, J. (2006). Numerical analysis of the enf test for mode ii wood fracture. *Composite Part A*, **37**, 1334–1344.
- Simon, F., & Valentin, G. (2000). Damage and fracture of wood adhesive joints under shear or opening loading. *5th European adhesion conference, EURADH'2000, Lyon, France*, **54**(296), 215–220.
- Simon, F., & Valentin, G. (2003). Cohesive failure characterisation of wood adhesive joints loaded in shear. *Fracture of Polymers, Composites and Adhesives II*, (pp. 395–316).
- Sjödín, J. (2008). Steel–to–timber dowel joints - influence of moisture induced stresses. Tech. Rep. nr. 31, Licentiate Thesis, Växjö University.
- Stanzl-Tschegg, S. E., Tan, D. M., & Tschegg, E. K. (1995). New splitting method for wood fracture characterization. *Wood Science and Technology*, **29**, 31–50.
- Vasic, S., Ceccotti, A., Smith, I., & J., S. (2009). Deformation rates effects in softwoods: Crack dynamics with lattice fracture modelling. *Eng. Frac. Mech.*, **76**, 1231–1246.
- Vasic, S., & Stanzl-Tschegg, S. (2007). Experimental and numerical investigation of wood fracture mechanisms at different humidity levels. *Holzforschung*, **61**, 367–374.
- Yoshihara, H. (2007). Simple estimation of critical stress intensity factors of wood by tests with double cantilever beam and three-point end notched flexure. *Holzforschung*, **61**, 182–189.
- Zhou, H., Zhu, E., Fortino, S., & Toratti, T. (2010). Modelling the hygrothermal stress in curved glulam beams. *Journal of Strain Analysis for Engineering Design*, **45**, 129–140.

Stefania Fortino
 VTT Technical Research Centre of Finland
 P.O.Box 1000, FIN-02044 VTT
 stefania.fortino@vtt.fi

Giuseppe Zagari, Antonio Lorenzo Mendicino
 University of Calabria
 Via P.Bucci, Cubo 39/b, 87036 Rende (CS), Italy
 gzagari@unical.it, antonio_lorenzo.mendicino@unical.it

Gerhard Dill-Langer
 MPA Stuttgart, Otto-Graf-Institut (FMPA)
 Abteilung Holzbau, Pfaffenwaldring 4b - 70569 Stuttgart, Germany
 gerhard.dill-langer@mpa.uni-stuttgart.de

Appendix. Short description of the Abaqus tools suitable for cohesive crack propagation in wood

Modelling of the cohesive zone

According to the notation used in (Abaqus, 2008), the stress state \mathbf{t} in the cohesive zone (CZ) in a general 3D context is defined as follows:

- Before damage initiation, the stress vector \mathbf{t} is linearly dependent on a certain stiffness matrix such that the CZ must have the same behaviour in the remaining part of the domain:

$$\mathbf{t} = \begin{bmatrix} t_n \\ t_s \\ t_t \end{bmatrix} = \begin{bmatrix} K_{nn} & K_{ns} & K_{nt} \\ K_{ns} & K_{ss} & K_{st} \\ K_{nt} & K_{st} & K_{tt} \end{bmatrix} \begin{bmatrix} \varepsilon_n \\ \varepsilon_s \\ \varepsilon_t \end{bmatrix} = \mathbf{K}\boldsymbol{\varepsilon} \quad (1)$$

where the nominal strain values in the normal, shear and tangential directions (with respect to the crack plane) are defined respectively as $\varepsilon_n = \delta_n/T_0$, $\varepsilon_s = \delta_s/T_0$, $\varepsilon_t = \delta_t/T_0$ being $\delta_n, \delta_s, \delta_t$ the separation displacements between corresponding points at the interface and T_0 the thickness of the cohesive element. Note that the model is not sensitive to these values of displacement and the largest one which does not produce numerical instability can be used. \mathbf{K} is the interface matrix containing the interface stiffness values. In this work uncoupling between normal and shear components is used by setting to zero the off-diagonal stiffness terms.

- During softening, \mathbf{t} is defined on the basis of a damage parameters matrix $\mathbf{D}(\delta_i)$:

$$\mathbf{t} = (\mathbf{I} - \mathbf{D}(\delta_i))\bar{\mathbf{t}}, \quad i = n, s, t \quad (2)$$

where \mathbf{I} is the identity matrix and \mathbf{D} is a diagonal matrix containing the damage parameters d_i as functions of the actual δ_i as well as $\delta_{i,\max} = \delta_{\max}$, that is the maximum separation displacement provided for the softening branch of the cohesive law. The parameters d_i are defined as $0 < d_i < 1$. In particular:

$$t_n = \begin{cases} (1 - D)\bar{t}_n, & \bar{t}_n \geq 0 \\ t_n & \text{otherwise} \end{cases} \quad (3)$$

$$t_s = (1 - D)\bar{t}_s \quad (4)$$

$$t_t = (1 - D)\bar{t}_t \quad (5)$$

- Out of the displacement range provided by the cohesive law, $\mathbf{t} = \mathbf{0}$.

The exponential softening, which is found to be suitable for both wood material and parametric studies, is the one suggested in (Abaqus, 2008):

$$D = 1 - \left\{ \frac{\delta_m^0}{\delta_m^{\max}} \right\} \left\{ 1 - \frac{1 - \exp\left(-\alpha \left(\frac{\delta_m^{\max} - \delta_m^0}{\delta_m^f - \delta_m^0} \right)\right)}{1 - \exp(-\alpha)} \right\} \quad (6)$$

where α is a damage parameter, $\delta_m = \sqrt{\langle \delta_n \rangle^2 + \delta_s^2 + \delta_t^2}$ is the effective displacement introduced in (Camanho & Davila, 2002) for general cases of damage under a combination

of normal and shear deformation across the interface, δ_m^0 is the effective displacement at damage initiation and δ_m^f the effective displacement at complete failure.

The cohesive material available in Abaqus and suitable for short-term opening mode analyses of wood is defined through the "TRACTION" option which describes the damage for traction separation law. By using this option, three stiffness values are needed which can be chosen to be up to $1e+3$ times the stiffness of the material attached to the cohesive zone in the same direction.

The "DAMAGE INITIATION CRITERION" and the "DAMAGE EVOLUTION TYPE" options have to be further selected. For the onset of damage, a tension-based criterion is found to be suitable so that the related Abaqus option refers to the maximum nominal traction stress. For the damage evolution, an energy criterion and an exponential law are selected. Furthermore, a linear elastic stiffness for simulating the behaviour of the material before onset of crack-growth is chosen such that the linear state is equal to that of the model without cohesive elements.

In the definition of "COHESIVE SECTION", the chosen "MAX DEGRADATION" parameter is 0.9. The element zone is discretized with at least $1/5$ length of the adjacent solid continuum elements.

Scripting tools

A Script file for a parametric study is composed of the following parts:

1. creation of a parametric study by using the Python command "aStudy";
2. definition of sets of values for the parameters T_{\max} , δ_{\max} and α by using the field command "aStudy.define";
3. definition of the number of parameters to be used in the analyses by the field command "aStudy.sample" and combination of the various tests by using the command "aStudy.combine";
4. definition of a constraint for the analysis by the command "aStudy.constrain" (in this case, the area under the traction-separation curve has to be equal to the fracture energy);
5. generation of the data by the "aStudy.generate" command and execution of all analysis jobs sequentially by the command "aStudy.execute".